Mode Ordering in Tuning Fork Structures with Negative Structural Coupling for Mitigation of Common-mode g-Sensitivity

Brenton R. Simon, Sambuddha Khan, Alexander A. Trusov, and Andrei M. Shkel
Microsystems Laboratory, Department of Mechanical and Aerospace Engineering,
University of California, Irvine, CA, USA
E-mail: brent.simon@gmail.com, sambuddk@uci.edu, alex.trusov@gmail.com, and ashkel@uci.edu

***Abstract*— This paper reports a method of mode ordering in tuning fork structures, effectively inducing a negative coupling stiffness between the resonant proof masses. The coupling mechanism selectively stiffens the undesirable in-phase resonance mode and softens the desirable out-of-phase resonance, thus widening the frequency separation between the desirable and undesirable modes of vibration in tuning fork structures. In gyroscopes, the approach leads to improved robustness to fabrication imperfections and immunity to environmental vibrations, while at the same time enhancing the scale factor and reducing the noise. Advantages of the method are illustrated on a Quadruple Mass Gyroscope (QMG) architecture, which was previously reported. It is experimentally demonstrated that the common-mode g-sensitivity can be reduced by over 20 times with design modifications resulting in mode re-ordering.**

Keywords—mode ordering, g-sensitivity, negative coupling stiffness, Coriolis Vibratory Gyroscopes.

I. Introduction

The noise and stability of high-performance micromachined inertial sensors such as gyroscopes and accelerometers are limited by the Quality factor (Q) of devices [1]. The mechanical scale factor of Coriolis vibratory gyroscopes, as well as amplitude modulated accelerometers, is inversely proportional to natural frequency of the devices. The Q-factor can be improved by reducing the natural resonance frequency and thereby reducing thermoelastic damping [1]. However, reduction of operational frequency increases the influence of external acceleration, which is a disadvantage for high-performance inertial sensors.

The influence of external common-mode acceleration can be minimized by using the anti-phase vibratory mode of the tuning fork resonators, without raising the natural frequency of the device. However, the in-phase vibratory mode is always the lower in frequency than the operational anti-phase mode, when conventional flexures are used. Such mode ordering [2] leads to a higher than desired anti-phase operational mode, which effectively reduces the mechanical scale factor. The design configuration also leaves the frequency of the in-phase vibratory mode lower in order of resonant frequencies, which is most sensitive to external acceleration, and most likely to respond to common-mode external acceleration.

In this paper, we demonstrate that mode ordering is necessary to improve the performance of inertial sensors. Our study includes both analytical modeling and experimental results. A dual-axis anti-phase tuning fork resonator is used for this purpose. Mode ordering is achieved by designing a suitable coupling structure that switches the in-phase and anti-phase resonances of the tuning fork resonator in the frequency spectrum. This leads to a low anti-phase resonance with a high mechanical scale factor, while pushing the acceleration-sensitive in-phase resonance to high frequencies, the frequencies of perturbation that the device is less likely to experience.

II. A Dual-Axis Anti-Phase Tuning Fork Resonator

A dual-axis tuning fork resonator with eight degrees of freedom uses the same design principals of a classic Coriolis vibratory gyroscope with a higher degree of symmetry. An example of a dual-axis tuning fork device is shown in Fig. 1.

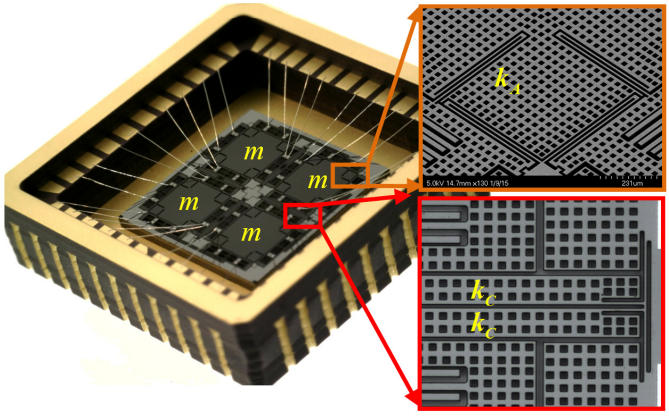

Fig. 1. An optical photograph of a fabricated and packaged QMG devices with SEM images of the supporting and coupling springs.

This is an in-house fabricated and packaged Quad-Mass-Gyroscope (QMG), [3]. As it can be seen in this image, the structure consists of four identical proof masses (individual

This work was supported by DARPA under grant N66001-12-C-4035.

mass, m), which are grounded to a substrate with supporting springs of an equal stiffness, k_A. The four proof masses are also mechanically coupled to their adjacent counterparts using mechanical coupling springs of value k_C, also shown in the Fig. 1.

A conceptual schematic of Fig. 1 is shown in Fig. 2. There are four primary mode shapes that are associated with the quad-mass tuning fork resonator, as shown in Fig. 1, including in-phase, anti-phase, opposing in-phase, and double anti-phase modes. While the in-phase mode is sensitive to acceleration, the opposing in-phase mode is particularity sensitive to external torque. This can be seen from Fig. 2. The resonance frequencies of each vibratory mode shapes can be expressed by

$$\omega_{\text{In-phase}} = \sqrt{\frac{k_A}{m}};\ \omega_{\text{Opposing In-phase}} = \sqrt{\frac{k_A}{m}}$$
$$\omega_{\text{Anti-phase}} = \sqrt{\frac{k_A + 2k_C}{m}};\ \omega_{\text{Double Anti-phase}} = \sqrt{\frac{k_A + 2k_C}{m}} \quad (1)$$

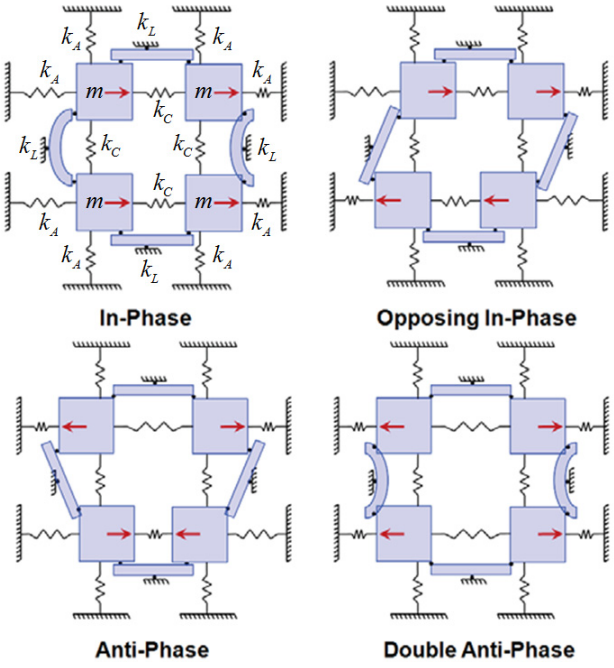

Fig. 2. Conceptual schematic of a double-axis tuning fork with external coupling levers.

For conventional spring coupling, the stiffness is always positive. This leads to anti-phase and double anti-phase vibratory modes that are always higher in frequency than the in-phase and opposing in-phase modes. In addition, the double-axis tuning fork contains degenerate mode shapes along each individual axis (i.e., $\omega_{\text{In-phase}} = \omega_{\text{Opposing In-phase}}$ and $\omega_{\text{Anti-phase}} = \omega_{\text{Double Anti-phase}}$). This effect leads to high energy coupling between each degenerate mode under static conditions. A reordering of the mode shapes using suitable coupling mechanisms is necessary to eliminate the excitation of undesirable modes.

III. Coupling Structures for Tailored Mode Ordering

In order to solve the mode ordering challenge, two techniques are implemented, including external lever coupling and internal lever coupling. These two techniques are presented next.

A. External Lever Coupling

In order to isolate each individual mode shape within the frequency spectrum, external levers are used, as shown in Fig. 2. The coupling beams are designed to be robust to translation, yet compliant to rotation. The levers behave as anti-phase stiffness elements, forcing the anti-phase motion of neighboring proof masses. The modal frequencies of such a system can be calculated as

$$\omega_{\text{In-Phase}} = \sqrt{\frac{k_A + 2k_L}{m}};\ \omega_{\text{Opposing In-Phase}} = \sqrt{\frac{k_A}{m}}$$
$$\omega_{\text{Anti-Phase}} = \sqrt{\frac{k_A + 2k_C}{m}};\ \omega_{\text{Double Anti-Phase}} = \sqrt{\frac{k_A + 2k_C + 2k_L}{m}} \quad (2)$$

Eq. (2) shows that with the inclusion of this additional design element the four primary modal frequencies can now be isolated from one another. The placement of these frequencies is still not ideal, though. Using the lever coupling method, $\omega_{\text{Opposing In-phase}}$ is now the vibratory mode with lowest frequency, which is still sensitive to an external torque. The simulated frequency spectrum of such a device is shown in Fig. 3a.

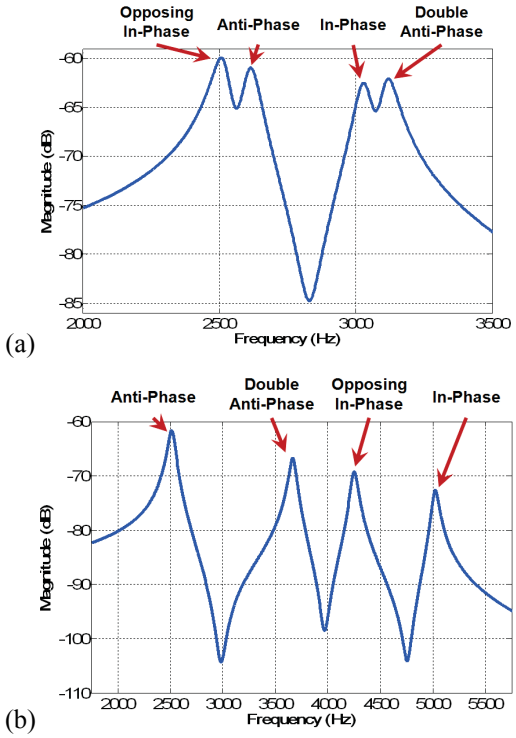

Fig. 3. Simulated frequency spectrums of a dual-axis tuning fork with (a) External lever only, (b) with both external levers and negative-stiffness internal levers

B. *Internal Lever Coupling*

Even though the external lever coupling is able to separate all the mode shapes of a quad-mass resonator, the placement of the modal frequencies is still not ideal. In this section, an alternative internal coupling mechanism with negative stiffness is applied between two proof masses, replacing the traditional beam springs with positive structural stiffness.

Eq. (2) shows that if k_C is designed to be negative ($k_C \le 0$) with positive values of k_A and k_L, the mode ordering changes, making the anti-phase mode to be the lowest of the four and the in-phase mode-shape to be the highest. Thus, the design requirement for rejection of common-mode acceleration is achieved. The frequency placement of all the mode shapes of the quad-mass resonator after mode-ordering using negative-stiffness internal levers is shown in Fig. 3b.

IV. Analytical Model of Internal Lever Coupling with Negative Stiffness

In order to create a negative coupling stiffness, a secondary resonator is introduced along with the primary tuning fork resonator to selectively stiffen the in-phase motion of the primary resonators with respect to the anti-phase motion. In this paper, the first two mode shapes of a simple clamped-clamped beam are used to create a negative coupling stiffness for the primary resonator. A schematic of this secondary resonator is shown in Fig. 4, along with a model of the equivalent parameters. Due to anchoring of the structure, an additional grounding stiffness is applied to each proof-mass, which increases the total individual stiffness applied to each mass: $k_A = k + k_{IN}$.

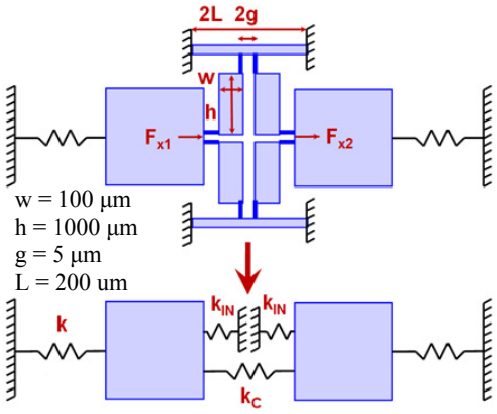

Fig. 4. Conceptual schematic of a negative stiffness coupling (top), along with an equivalent mass-spring system (bottom).

Fig. 4 also shows the critical dimensions of one-half of the coupling structure. The coupling structure is formed with two parts: 1) levers with dimensions w and h, which are used to transform the displacement of the proof-masses, and 2) a clamped-clamped beam, which absorbs this transformed displacement. The in-phase and anti-phase resonances of the primary structure excite two different mode shapes within the secondary resonator. These mode shapes are shown in Fig. 5(a-b).

For anti-phase motion of the proof masses, the clamped-clamped beam is forced in the same direction by the proof masses, but torqued in opposite directions, Fig. 5a. For in-phase motion, the clamped-clamped beam is forced in opposite directions by the proof masses, but torqued in the same direction, Fig. 5b. Because an anti-phase resonance of the primary structure forces the first mode shape of the beam, while an in-phase resonance forces the second mode shape, it can be intuitively seen that the in-phase resonance will have a higher stiffness.

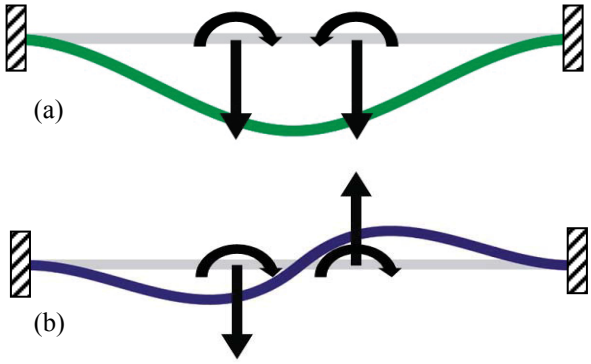

Fig. 5. Mode shapes of a clamped-clamped beam used as a coupling structure, (a) the first mode shape or the lowest frequency mode is excited during the anti-phase motion of the primary resonator; (b) the second mode shape with higher frequency is excited during the in-phase motion of the primary resonator.

In order to confirm and quantify this variability in stiffness, analytical expressions for the anti-phase and in-phase stiffness of the coupling structure were calculated with respect to motion of the primary resonator. The results are shown in Eqs. (3) and (4) for the anti-phase and in-phase mode shapes, respectively.

$$k_{\text{Anti-Phase}} = \left[\frac{(L-g)^2 h}{EI(2L)^3 w} \left[\frac{wh}{w^2+h^2} \frac{2}{3} L^2 \cdot (L-g) \cdot (L+3g) + h\left(4gL^2\right) \right] \right]^{-1} \quad (3)$$

$$k_{\text{In-Phase}} = \left[\frac{(L-g)^2 h}{EI(2L)^3 w} \left[\frac{wh}{w^2+h^2} \frac{2}{3} g^2 (L-g)(3L+g) + h\left(2gL^2 - 4Lg^2 - 2g^3\right) \right] \right]^{-1} \quad (4)$$

When $(k_{\text{Anti-phase}}/k_{\text{In-phase}}) < 1$, k_C is negative, which effectively forces the in-phase motion of the proof masses to be stiffer than the anti-phase motion. By plotting the k_C value versus L/g for various values of g, Fig. 6, it can be seen that for $L/g = 1$, $k_C = -k$. As L/g increases, k_C quickly becomes less negative as it approaches $k_C = -0.25 \cdot k$. Then, as a function of h, w and g, k_C starts becoming more negative again, approaching a value of $k_C = -0.5 \cdot k$.

V. Experimental Results

In this section, the effect of negative coupling stiffness for gyroscope mode ordering and rejection of common-mode acceleration is demonstrated with experimental results.

Two nearly identical single-axis tuning fork devices were experimentally tested, one with a traditional spring coupling structure and another with the described lever coupling. Both resonators were fabricated using the SOI fabrication process and vacuum packaged using the process described in [4]. The only substantial difference in the design of the two resonators was how the masses were coupled. The resonator with the spring coupling was shown to have an anti-phase resonance frequency of 2.16 kHz, along with an in-phase frequency of 2.03 kHz. A resonator with the lever coupling had an anti-phase resonance frequency of 1.80 kHz, along with an in-phase frequency of 3.02 kHz. In order to quantify their degree of sensitivity to external acceleration, both devices were placed on a linear shaker and given a precise amplitude of vibration of 4g at 100 Hz along the sense-mode of the resonator. The frequency spectrum of the output of the resonator was recorded.

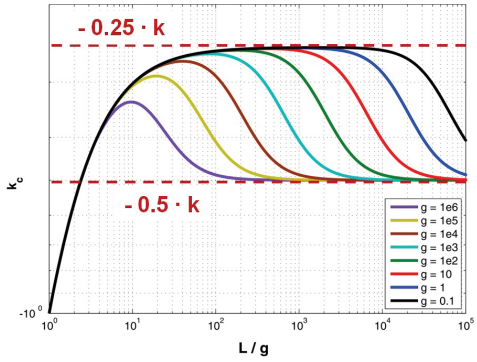

Fig. 6. Plot of the value of the equivalent coupling spring (k_C) versus (L/g) for h = 1000 μm and w = 100 μm.

By centering the frequency spectrum upon the operational frequency of the resonator, sidebands appear within this spectrum, set at a frequency offset of plus and minus the frequency of the external acceleration. The difference in magnitude between the primary resonance peak and the sidebands can then be used to identify the acceleration sensitivity according to Eq. (5), [5].

$$L(f_V) = 20\log_{10}\left(\left(\bar{\Gamma} \bullet \bar{a}\right) \cdot f / 2f_V\right), \qquad (5)$$

where, f_V and $\bar{a}$ are the frequency and amplitude of the physical vibration, f is the frequency of the resonator, and $\bar{\Gamma}$ is the acceleration sensitivity of the resonator.

The frequency spectrums of both resonators along with the side bands are shown in Fig. 7. As can be seen from these results, the magnitude between the primary resonance and sidebands was 82 dB for the spring coupled device and 110 dB for the negative-stiffness-lever coupled resonator. Using Eq. (5), this corresponds to acceleration sensitivities of 2×10^{-6} g^{-1} and 9×10^{-8} g^{-1}, respectively. Therefore, the negative-stiffness-lever coupling has been shown to improve the common-mode acceleration rejection by approximately 22 times.

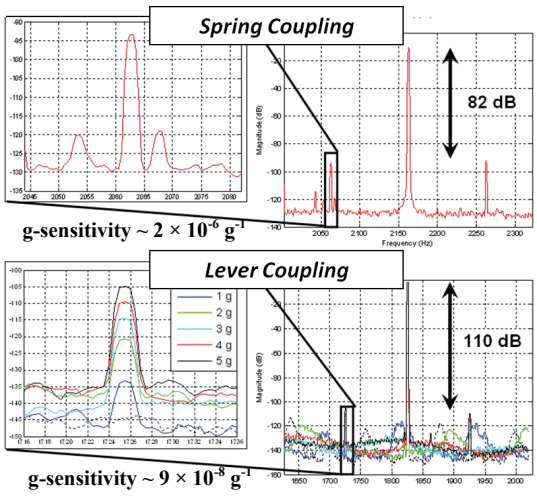

Fig. 7. Experimental g-sensitivity data of two resonators illustrating advantages of the method.

VI. Conclusions

Resonant MEMS structures fundamentally have a potential for higher performance due to their lower operational frequencies and high amplitudes of motion. A significant disadvantage to this, however, is an acceleration sensitivity or g-sensitivity.

In this paper, we investigated a method for mitigation of this sensitivity by using the mode ordering of anti-phase resonances, using as an example the quad-mass tuning fork structures. Mode ordering is accomplished by raising the in-phase frequency as high as possible, while leaving the useful anti-phase frequency low in the order of resonance modes. In this paper, a novel coupling structure is introduced that is capable of accomplishing this goal, which is believed to achieve the highest in-phase / anti-phase frequency separation of a tuning fork structure to date. This structure has also been shown experimentally to reduce the acceleration sensitivity by over 20 times, which is consistent with predicted results.

References

[1] S.A. Zotov, B.R. Simon, I.P. Prikhodko, A.A. Trusov, A.M. Shkel, "Quality Factor Maximization through Dynamic Balancing of Tuning Fork Resonator," IEEE Sensors Journal, Vol. 14, No. 8, 2014.

[2] B.R. Simon, A.A. Trusov, A.M. Shkel, "Anti-Phase Mode Isolation in Tuning-Fork MEMS Using a Lever Coupling Design," IEEE Sensors 2012, October 2012.

[3] A. A. Trusov, A. R. Schofield, and A. M. Shkel, "Micromachined Tuning Fork Gyroscopes with Ultra-High Sensitivity and Shock Rejection," US Patent 8,322,213.

[4] Alexander A. Trusov, Adam R. Schofield, Andrei M. Shkel, "Micromachined rate gyroscope architecture with ultra-high quality factor and improved mode ordering," Sensors and Actuators A: Physical, Vol. 165, Issue 1, pp. 26-34, January 2011.

[5] R.L. Filler, "The Acceleration Sensitivity of Quartz Crystal Oscillators: Review,"IEEE Transactions on Ultrasonics, Ferroelectrics and frequency Control, Vol. 35, No.3, 1988.